

**Tetranuclear Coordination Assemblies Based on Half-sandwich Ruthenium(II) Complexes. Non Covalent Binding to DNA and Cytotoxicity**

Journal:	<i>Inorganic Chemistry</i>
Manuscript ID:	ic-2009-00980y.R1
Manuscript Type:	Article
Date Submitted by the Author:	23-Jun-2009
Complete List of Authors:	Navarro, Jorge; Universidad de Granada, Departamento Quimica Inorganica Linares, Fatima; Universidad de Granada Galindo, Miguel; Univ. Newcastle Romero, Maria; Universidad de Granada, Departamento Quimica Inorganica Galli, Simona; Università dell'Insubria, Dipartimento di Scienze Chimiche e Ambientali Barea, Elisa; Universidad de Granada



1  
2  
3  
4  
5  
6  
7  
8  
9  
10  
11  
12  
13  
14  
15  
16  
17  
18  
19  
20  
21  
22

# Tetranuclear Coordination Assemblies Based on Half-sandwich Ruthenium(II) Complexes. Non Covalent Binding to DNA and Cytotoxicity

23  
24  
25  
26  
27  
28  
29  
30  
31  
32

*Fátima Linares,<sup>a</sup> Miguel A. Galindo,<sup>b</sup> Simona Galli,<sup>c</sup> M. Angustias Romero,<sup>a</sup> Jorge A. R. Navarro<sup>a,\*</sup> and Elisa Barea<sup>a,\*</sup>*

33  
34  
35  
36  
37  
38

<sup>a</sup>Departamento de Química Inorgánica, Universidad de Granada, Av. Fuentenueva S/N, 18071 Granada (Spain)

39  
40  
41  
42  
43  
44  
45  
46  
47  
48  
49  
50  
51  
52  
53  
54  
55  
56  
57  
58  
59  
60

<sup>b</sup>School of Chemistry, Newcastle University, Bedson Building, Newcastle Upon Tyne, NE1 7RU, UK

<sup>c</sup>Dipartimento di Scienze Chimiche e Ambientali, Università dell'Insubria, Via Valleggio 11, 22100 Como, Italy.

E-mail: ebaream@ugr.es, jarn@ugr.es

**RECEIVED DATE (to be automatically inserted after your manuscript is accepted if required according to the journal that you are submitting your paper to)**

**ABSTRACT**

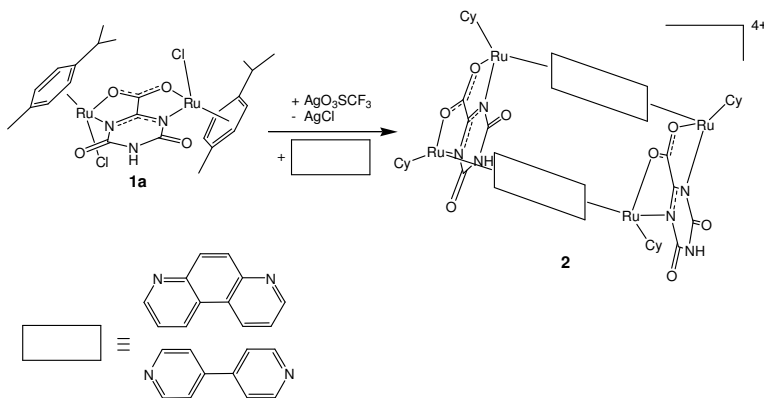
The reaction of [(cymene)RuCl<sub>2</sub>]<sub>2</sub> with K<sub>2</sub>Hoxonate (H<sub>3</sub>oxonic: 4,6-dihydroxy-2-carboxy-1,3,5-triazine acid) in methanol leads to the formation of the dinuclear half-sandwich ruthenium(II) complex [(cymene)<sub>2</sub>Ru<sub>2</sub>(μ-Hoxonato)Cl<sub>2</sub>] (**1a**). Removal of the chloride ligands of **1a** by treatment with AgCF<sub>3</sub>SO<sub>3</sub> yields [(cymene)<sub>2</sub>Ru<sub>2</sub>(μ-Hoxonato)(CF<sub>3</sub>SO<sub>3</sub>)<sub>2</sub>] (**1b**) which, upon posterior reaction with *N,N'*-linkers (L = 4,4'-bipyridine (4,4'-bpy), 4,7-phenantroline (4,7-phen)), gives rise to the formation of the tetranuclear open boxes [(cymene)<sub>4</sub>Ru<sub>4</sub>(μ-Hoxonato)<sub>2</sub>(μ-*N,N'*-L)<sub>2</sub>](CF<sub>3</sub>SO<sub>3</sub>)<sub>4</sub> (**2a**: L = 4,4'-bpy; **2b**: L = 4,7-phen). These systems have been characterised by <sup>1</sup>H NMR, UV-vis and ESI-MS. The single crystal structures of the dinuclear precursor **1a** and of the clathrate **2b**·**4,7-phen** have been determined. The interaction of these systems with cysteine, mononucleotides and calf-thymus DNA has been studied by means of <sup>1</sup>H NMR, UV-vis, circular dichroism, competitive binding assays and AFM imaging. The results show that the robust tetracationic ruthenium(II) cyclic systems **2a** and **2b** do not give ligand exchange reactions towards biorelevant ligands. Nevertheless, these systems are able to non-covalently bind to DNA, probably at the surface the major groove, inducing significant conformational changes in this biomolecule. It is also interesting to note that compounds **2a** and **2b**, in spite of only giving supramolecular interactions with biomolecules, exhibit antitumor activity, particularly, towards the human ovarian cancer cell line A2780*cisR*, showing acquired resistance to *cisplatin*, with respective 4.6 and 8.3 microM IC<sub>50</sub> values.

**KEYWORDS.** Antitumor agents · bioorganometallic chemistry · bioinorganic chemistry · coordination cages · supramolecular chemistry.

## INTRODUCTION

1  
2  
3 The unwished side effects of the treatment of cancer patients with *cisplatin* and related metallodrugs<sup>1</sup>  
4  
5 have prompted the research of alternative systems with a different chemical nature. In this regard, the  
6  
7 organometallic half-sandwich ruthenium(II) complexes of the type  $[(\eta^6\text{-arene})\text{Ru}(\text{YZ})(\text{X})]$ , where YZ is,  
8  
9 typically, a chelating ligand and X is a halide, are currently the subject of interest as a result of their *in*  
10  
11 *vitro* and *in vivo* anticancer activity.<sup>2</sup> Although, like *cisplatin*, these systems have also shown to give rise  
12  
13 to coordinative binding to DNA (through N7 of guanine),<sup>3,4</sup> their biological chemistry is quite  
14  
15 different.<sup>4,5</sup> It is also interesting to note the recent report of Therrien and col. on the ability of a half-  
16  
17 sandwich ruthenium based coordination cage to encapsulate  $[\text{M}(\text{acac})_2]$  ( $\text{M} = \text{Pt}^{2+}, \text{Pd}^{2+}$ ) complexes with  
18  
19 a synergic enhancement of their antitumor activity.<sup>6</sup> On the other hand, we and others have shown that  
20  
21 polynuclear coordination assemblies like iron(II)<sup>7</sup> and ruthenium(II) helicates,<sup>8</sup> as well as platinum(II)  
22  
23 Fujita's coordination squares<sup>9</sup> and metallacalixarenes,<sup>10,11</sup> non-covalently bind to DNA with a  
24  
25 concomitant biological effect (i.e. antitumor activity, telomerase inhibition). Likewise, Fujita and col.  
26  
27 have very recently reported the isolation effect exerted by Pt(II) coordination cages which strongly  
28  
29 stabilize the minimal nucleotide duplex formation in highly competitive aqueous solutions.<sup>12</sup>  
30  
31  
32  
33  
34

35  
36 The above mentioned results prompted us to study new examples of systems able to give  
37  
38 unconventional interactions with biomolecules in order to find out new ways to overcome some  
39  
40 problems encountered with classical metallodrugs. In this manuscript, we show a strategy to build a  
41  
42 series of cationic cyclic polynuclear half-sandwich ruthenium(II) complexes complexes of the  
43  
44  $[(\text{cymene})_4\text{Ru}_4(\mu\text{-Hoxonato})_2(\mu\text{-}N,N'\text{-L})_2](\text{CF}_3\text{SO}_3)_4$  kind (**2a**: L = 4,4'-bpy; **2b**: L= 4,7-phen),  
45  
46 containing Hoxonato bridges (H<sub>3</sub>oxonic: 4,6-dihydroxy-2-carboxy-1,3,5-triazine acid) and *N,N'*-linkers  
47  
48 (4,4'-bipyridine (4,4'-bpy), 4,7-phenanthroline (4,7-phen)) (Scheme 1). In addition, we have essayed the  
49  
50 interaction of these systems with DNA and their citotoxic activity towards human lung and ovarian  
51  
52 tumor cell lines. We have chosen the Hoxonato system with the purpose of creating a  $\pi$ -acidic surface  
53  
54 able to give specific interactions with nucleotides through anion- $\pi$  interactions<sup>13</sup> and complementary H-  
55  
56 bonding interactions.<sup>14</sup>  
57  
58  
59  
60



**Scheme 1.** Formation reaction of the  $[(\text{cymene})_4\text{Ru}_4(\text{Hoxonato})_2(N,N'\text{-L})_2](\text{CF}_3\text{SO}_3)_4$  (**2a**: L = 4,4'-bpy; **2b**: L = 4,7-phen) cyclic assemblies.

## EXPERIMENTAL

### Materials

$[(\eta^6\text{-p-cymene})\text{Ru}(\text{Cl})_2]_2$  was prepared according to literature methods.<sup>15</sup> Oxonic acid potassium salt ( $\text{KH}_2\text{oxonate}$ ), 4,4'-bipyridine (4,4'-bpy) and 4,7-phenanthroline (4,7-phen) were acquired from commercial sources and used as received.

### Synthesis

**$[(\text{cymene})_2\text{Ru}_2\text{Cl}_2(\text{Hoxonato})]$  (1a):**  $[(\eta^6\text{-p-cymene})\text{Ru}(\text{Cl})_2]_2$  (612 mg, 1.0 mmol) and oxonic acid potassium salt (195 mg, 1 mmol) were suspended in methanol (30 mL). KOH (40 mg, 0.7 mmol) was added to the suspension and the resulting mixture was refluxed at 70 °C for 6h to give, upon cooling, an orange precipitate which was filtered off. Crystals suitable for X-ray diffraction were obtained by slow evaporation of a  $\text{CHCl}_3$  solution (544 mg, 78.1% yield).  $^1\text{H}$  NMR (400 MHz,  $\text{DMSO-d}_6$ , 25 °C):  $\delta$  (ppm) = 1.08 (m, 12H,  $\text{CH}_3\text{-cymene}$ ), 2.07 (s, 6H,  $\text{CH}_3\text{-cymene}$ ), 2.65 (m, 2H,  $\text{CH-cymene}$ ), 5.58 (d, 2H, aromatic H-cymene), 5.71 (d, 2H, aromatic H-cymene), 5.81 (d, 2H, aromatic H-cymene), 5.92 (d, 2H, aromatic H-cymene), 11.80 (s, 1H,  $\text{NH-oxonatoH}$ ); elemental analysis calcd (%) for  $\text{C}_{24}\text{H}_{31}\text{N}_3\text{O}_4\text{Cl}_2\text{Ru}_2$ : C 41.26, H 4.47, N 6.02; found: C 41.06, H 4.11, N 6.02.

1 [(cymene)<sub>2</sub>Ru<sub>2</sub>(CF<sub>3</sub>SO<sub>3</sub>)<sub>2</sub>(Hoxonato)]<sub>2</sub> (**1b**): Solid Ag(CF<sub>3</sub>SO<sub>3</sub>) (2 mmol, 513 mg) was added to a  
2 suspension of [(cymene)<sub>2</sub>Ru<sub>2</sub>Cl<sub>2</sub>(Hoxonato)] (**1a**) (1 mmol, 696 mg) in methanol. The mixture was  
3 stirred in the dark at 40 °C for 120 min. Subsequent filtration of AgCl led to isolate an orange solution  
4 which contained the expected compound. (795 mg, 82.6% yield). <sup>1</sup>H NMR (400 MHz, DMSO-d<sub>6</sub>, 25  
5 °C): δ (ppm) = 1.10 (m, 12H, CH<sub>3</sub>-cymene), 2.08 (m, 6H, CH<sub>3</sub>-cymene), 2.63 (m, 2H, CH-cymene), 6.06  
6 (m, 7H, aromatic H-cymene), 6.45 (m, 1H, aromatic H-cymene), 11.87 (s, 1H, NH-oxonatoH);  
7 elemental analysis calcd (%) for C<sub>26</sub>H<sub>31</sub>N<sub>3</sub>O<sub>10</sub>S<sub>2</sub>F<sub>6</sub>Ru<sub>2</sub>: C 32.53, H 3.47, N 4.38, S 6.68; found: C 31.29,  
8 H 3.33, N 4.25, S, 7.21.  
9

10 [(cymene)<sub>4</sub>Ru<sub>4</sub>(Hoxonato)<sub>2</sub>(4,4'-bpy)<sub>2</sub>](CF<sub>3</sub>SO<sub>3</sub>)<sub>4</sub>(H<sub>2</sub>O)<sub>3</sub> (**2a**): Solid 4,4'-bipyridine (1 mmol, 156  
11 mg) was added to a solution of compound **1b** (1 mmol in 15 mL of MeOH). The resulting solution was  
12 stirred at room temperature for 24h and then was let stand. After one day, an orange precipitate of **2a**  
13 was isolated. (670 mg, 60.4% yield). <sup>1</sup>H NMR (400 MHz, DMSO-d<sub>6</sub>, 25 °C): δ (ppm) = 1.15 (dd, 12H,  
14 CH<sub>3</sub>-cymene), 1.71 (s, 6H, CH<sub>3</sub>-cymene), 2.70 (m, 2H, CH-cymene), 5.90 (d, 4H, aromatic H-cymene),  
15 6.22 (d, 4H, aromatic H-cymene), 7.65 (d, 4H, 4,4'-bpy), 8.06 (d, 4H, 4,4'-bpy), 12.58 (s, 1H, NH-  
16 oxonatoH); FTMS (+ESI): m/z; 931.05 [M - 2CF<sub>3</sub>SO<sub>3</sub>]<sup>2+</sup>. Elemental analysis calcd (%) for  
17 C<sub>72</sub>H<sub>80</sub>N<sub>10</sub>O<sub>23</sub>S<sub>4</sub>F<sub>12</sub>Ru<sub>4</sub>: C 39.06, H 3.64, N 6.33, S 5.79; found: C 38.60, H 3.88, N 6.37, S, 6.27.  
18

19 [(cymene)<sub>4</sub>Ru<sub>4</sub>(oxonatoH)<sub>2</sub>(4,7-phen)<sub>2</sub>](CF<sub>3</sub>SO<sub>3</sub>)<sub>4</sub>(CH<sub>3</sub>OH) (**2b**): To a solution of compound **1b** (1  
20 mmol in 15 mL of MeOH), was added solid 4,7-phenanthroline (1 mmol, 180 mg). The mixture was  
21 stirred for 24h to give an orange solid of **2b**. (451mg, 40.8% yield). <sup>1</sup>H NMR (400 MHz, DMSO-d<sub>6</sub>, 25  
22 °C): δ (ppm) = 1.12 (dd, 6H, CH<sub>3</sub>-cymene), 1.28 (dd, 6H, CH<sub>3</sub>-cymene), 1.58 (s, 6H, CH-cymene),  
23 2.07 2.72 (m, 2H, CH-cymene), 5.94 (d, 2H, aromatic H-cymene), 6.19 (d, 2H, aromatic H-cymene),  
24 6.28 (d, 2H, aromatic H-cymene), 6.52 (d, 2H, aromatic H-cymene), 7.55 (s, 2H, 4,7-phen), 7.69 (m,  
25 1H, 4,7-phen), 8.07 (s, 2H, 4,7-phen), 8.32 (s, 2H, 4,7-phen), 8.80 (s, 1H, 4,7-phen), 9.07 (s, 2H, 4,7-  
26 phen), 9.18 (d, 1H, 4,7-phen), 12.80 (s, 1H, NH-oxonatoH); FTMS (+ESI): m/z; 955.05 [M -  
27 2CF<sub>3</sub>SO<sub>3</sub>]<sup>2+</sup>. Elemental analysis calcd (%) for C<sub>77</sub>H<sub>78</sub>N<sub>10</sub>O<sub>21</sub>S<sub>4</sub>F<sub>12</sub>Ru<sub>4</sub>: C 41.29, H 3.51, N 6.25, S 5.73;  
28 found: C 42.46, H 3.74, N 6.58, S, 6.11.  
29  
30  
31  
32  
33  
34  
35  
36  
37  
38  
39  
40  
41  
42  
43  
44  
45  
46  
47  
48  
49  
50  
51  
52  
53  
54  
55  
56  
57  
58  
59  
60

1 Crystals of **2b**-**4,7-phen** suitable for X-ray diffraction were grown from a MeOH solution of **2b** in  
2 the presence of an excess of 4,7-phen.  
3

#### 4 *Characterisation and physical measurements*

5  
6  
7 The <sup>1</sup>H NMR experiments carried out for characterizing compounds **1a**, **1b**, **2a** and **2b** and for  
8 studying the interaction between cyclic systems, nucleotides and cysteine were performed in D<sub>2</sub>O and  
9 DMSO-d<sub>6</sub> solutions with 10 mg of compound and 0.75 mL of solvent. High temperature experiments  
10 were run in DMSO-d<sub>6</sub> with the aim of studying the conformational flexibility of the cyclic systems. <sup>1</sup>H  
11 NMR spectra were recorded with a BRUKER ARX 400 (400 MHz) (Centre of Scientific  
12 Instrumentation of the University of Granada). ESI-MS measurements were performed dissolving the  
13 samples in methanol and measuring on a Waters Micromass LCT Premier mass spectrometer. Elemental  
14 (C, H, N) analyses were obtained at a FISIONS-CARLO ERBA EA 1008 analyzer in the Centre of  
15 Scientific Instrumentation of the University of Granada. Molecular geometries of compounds **2a** and **2b**  
16 were optimised with Molecular Mechanics (MMFF) by using Spartan'04 program package  
17 (Wavefunction Inc.).  
18  
19  
20  
21  
22  
23  
24  
25  
26  
27  
28  
29  
30  
31  
32

#### 33 *X-ray crystallography*

34  
35  
36 Table 1 summarises the crystallographic data for **1a** and **2b**-**4,7-phen**. The single crystal X-ray  
37 diffraction data for species **1a** were acquired at room temperature from an orange platelet single crystal  
38 of approximate 0.10×0.10×0.05 mm dimensions, on an Enraf Nonius CAD4 automated diffractometer  
39 using graphite-monochromated Mo K $\alpha$  radiation ( $\lambda = 0.71073 \text{ \AA}$ ). The unit cell was determined on the  
40 basis of the setting angles of 25 randomly distributed reflections in the  $9.5 < \theta < 14.4^\circ$  range. The data  
41 collection was performed in the  $3.0 < \theta < 25.3^\circ$  range by applying the  $\omega$ -scan mode [ $\Delta\omega = 1.1 +$   
42  $(0.35 \tan\theta)$ ]. A total of 4678 unique and 3025 observed [ $I > 2\sigma(I)$ ] reflections were collected [ $R(\text{int}) =$   
43  $0.008$ ,  $R(\text{sigma}) = 0.085$ ], and used for the structure solution and the structure refinement (against 316  
44 parameters). The data were corrected for absorption<sup>16</sup> and Lorenz-polarization effects. The structure was  
45 solved by direct methods<sup>17</sup> and refined by full-matrix least-squares on  $F^2$ .<sup>18</sup> All the non-hydrogen atoms  
46  
47  
48  
49  
50  
51  
52  
53  
54  
55  
56  
57  
58  
59  
60

1 were refined anisotropically. Hydrogen atoms were made riding their parent atoms with an isotropic  
2 temperature factor 1.2 times that of their parent atoms.  
3

4  
5 The single crystal X-ray diffraction data for species **2b-4,7-phen** were acquired at 100 K from an  
6 orange prism single crystal of approximate 0.24×0.18×0.14 mm dimensions, on a Bruker APEX  
7 automated diffractometer using graphite-monochromated Mo K $\alpha$  radiation ( $\lambda = 0.71073 \text{ \AA}$ ). The data  
8 collection was performed in the  $1.14 < \theta < 26.4^\circ$  range by applying the  $\omega$ -scan mode. A total of 19586  
9 unique and 18078 observed [ $I > 2\sigma(I)$ ] reflections were collected [ $R(\text{int}) = 0.056$ ,  $R(\text{sigma}) = 0.036$ ], and  
10 used for the structure solution and the structure refinement (against 1125 parameters). The data were  
11 corrected for absorption<sup>19</sup> and Lorenz-polarization effects. The structure was solved by direct methods<sup>17</sup>  
12 and refined by full-matrix least-squares on  $F^2$ .<sup>18</sup> All the non-hydrogen atoms were refined  
13 anisotropically, but those of the solvent and of the triflate anions (S excluded). Hydrogen atoms were  
14 made riding their parent atoms with an isotropic temperature factor 1.2 times that of their parent atoms.  
15 The measured single crystal was twinned (with 0.72:0.28 refined components ratio). A rotational  
16 disorder of the CF<sub>3</sub> and SO<sub>3</sub> groups severely affected the triflate anions, an annoying but expected, and  
17 well documented, phenomenon. The disorder determined the presence of non negligible peaks of  
18 electron density nearby the triflate anions. Attempts to reasonably model this disorder were not  
19 successful. Nevertheless, it is worth noting that its presence does not affect the structural features of the  
20 Ru(II) tetranuclear complex.  
21  
22  
23  
24  
25  
26  
27  
28  
29  
30  
31  
32  
33  
34  
35  
36  
37  
38  
39  
40  
41  
42

43 Crystallographic data (excluding structure factors) for species **1a** and **2b-4,7-phen** have been  
44 deposited with the Cambridge Crystallographic Data Centre as supplementary publication no.s 714114-  
45 714115. Copies of the data can be obtained, free of charge, on application to CCDC, 12 Union Road,  
46 Cambridge CB2 1EZ, UK, (fax: +44-(0)1223-336033 or e-mail: deposit@ccdc.cam.ac.uk).  
47  
48  
49  
50  
51

#### 52 *DNA binding studies*

53  
54  
55 Calf-thymus DNA (ct-DNA) was purchased from Sigma/Aldrich. The ct-DNA was dissolved in water  
56 without any further purification and kept frozen until the day of the experiment. The ct-DNA  
57 concentration (moles of bases per litre) was determined spectroscopically by using the molar extinction  
58  
59  
60



1 coefficients at the maximum of the long-wavelength absorbance (ct-DNA  $\epsilon_{258}=6600 \text{ cm}^{-1}\text{mol}^{-1}\text{dm}^3$ ).  
2  
3 Concentrations of stock solutions of compounds **1b**, **2a** and **2b** were determined from accurately  
4 weighed samples of these materials. A stock sodium cacodylate buffer (100 mM) was prepared by  
5 mixing a 50 mL solution of sodium cacodylate (0.2 M, 4.24 g of  $\text{Na}(\text{CH}_2)_2\text{AsO}_2 \cdot 3\text{H}_2\text{O}$  in 100 mL) with  
6 9.3 mL of hydrochloric acid (0.2 M), and diluting to a total of 100 mL. Stock solutions of **1b**, **2a** and **2b**  
7 (500  $\mu\text{M}$ ) were prepared. All ct-DNA experiments were conducted in sodium cacodylic buffer (1 mM)  
8 and NaCl (20 mM). Spectroscopic titration series experiments keeping the ct-DNA concentration  
9 constant were undertaken by adding the salt, buffer, water and the cyclic assembly to the ct-DNA. The  
10 circular dichroism (CD) spectra were produced by using a Jasco J-715 spectropolarimeter. UV-Vis was  
11 performed and visualized by ThermoSpectronic UV300 using 2 mL of an aqueous solution of ct-DNA  
12 (150  $\mu\text{M}$ ) in NaCl (20mM) and sodium cacodylate buffer (1 mM). The previously described solutions  
13 were used to register the UV/Vis spectra adding increased quantities of compounds **2a** and **2b** and  
14 keeping the ct-DNA concentration constant (ct-DNA/metal-complexes mixing ratios range from 200:1  
15 to 5:1).  
16  
17  
18  
19  
20  
21  
22  
23  
24  
25  
26  
27  
28  
29  
30  
31  
32

33 Ethidium bromide (EB) displacement by the cyclic assemblies was calculated by measuring the  
34 quenching of the EB fluorescence as it leaves the protection of the ct-DNA. A ct-DNA/salts/buffer  
35 solution with EB (ct-DNA/EB 4:5, 4 mM:5 mM) was prepared. The emission spectrum was recorded as  
36 a function of **1b**, **2a** and **2b** concentration by using a Variant mod. Cary Eclipse Luminescence  
37 spectrometer and the ruthenium complex concentration was slowly increased for ct-DNA/metal-  
38 complex ratios from 70:1 to 1:1 keeping the ct-DNA and EB concentrations constant. After each  
39 addition the fluorescence and UV-visible spectra were recorded (parameters: emission: 600 nm;  
40 excitation: 540 nm; excitation slit: 10.0 nm; emission slit:15.0 nm).  
41  
42  
43  
44  
45  
46  
47  
48  
49  
50  
51

#### 52 *Atomic force microscopy imaging (AFM)*

53  
54 Adsorption of blank calf thymus DNA: Samples were prepared by depositing a drop (10  $\mu\text{L}$ ) of a  
55 ct-DNA solution (30  $\mu\text{M}$ ) containing  $\text{MgCl}_2$  (4 mM) onto a mica sheet. After adsorption for 1 min at  
56 room temperature, the samples were gently rinsed with milli-Q quality water and dried with nitrogen.  
57  
58  
59  
60

1 Adsorption of ct-DNA-complexes: Incubation of ct-DNA with **2a** and **2b**: Solutions of ct-DNA (30  
2  $\mu\text{M}$ ) containing  $\text{MgCl}_2$  (4 mM) were incubated at room temperature with **2a** and **2b** (3  
3 basepairs/complex) for one hour. A drop of these solutions (10  $\mu\text{L}$ ) was deposited onto a sheet of mica  
4 for 1 min. The samples were rinsed and dried as described above. AFM imaging: AFM imaging was  
5 performed in air by using Tapping Mode on a Multimode Nanoscope IIIa (Veeco, Metrology group) and  
6 NanoProbe tips (Veeco Inc.). Vibrational noise was reduced with an isolation system (Manfrotto).  
7  
8  
9

#### 10 *Biological assays*

11 Cytotoxic studies were performed at the UNIDAD DE EVALUACIÓN DE ACTIVIDADES  
12 FARMACOLÓGICAS, Instituto de Farmacia Industrial, Facultad de Farmacia, University of Santiago  
13 de Compostela 15782 Santiago de Compostela, SPAIN. The tumor cell lines A2780, A2780cisR, were  
14 cultured at 37 °C in RPMI 1640 medium (Gibco) supplemented with 10% FBS (Fetal Bovine Serum)  
15 and L-Glutamine 2 mM in an atmosphere of 95% of air and 5%  $\text{CO}_2$ . Cell death was evaluated by using  
16 a system based on the tetrazolium compound MTT [3-(4,5-dimethyl-2-thiazolyl)-2,5-diphenyl-  
17 2Htetrazolium bromide], which is reduced by living cells to yield a soluble formazan product that can be  
18 detected colorimetrically. Cells were seeded in 96-well sterile plates at a density of 4000 cells/ well in  
19 100  $\mu\text{L}$  of medium and were incubated 24 h. Complexes dissolved in DMSO were added to final  
20 concentrations ranging from 0 to  $1.1 \cdot 10^{-4}$  M in a volume of 100  $\mu\text{L}$ /well. The final concentration of  
21 DMSO in cell culture was maintained in all cases at 1%. 96 h later, 10  $\mu\text{L}$  of a freshly diluted MTT  
22 solution (2.5 mg/mL) was pipetted into each well and the plate was incubated at 37 °C in a humidified  
23 5%  $\text{CO}_2$  atmosphere. After 5 h, the medium was removed and the obtained formazan product was  
24 dissolved in 100  $\mu\text{L}$  of DMSO. The cell viability was evaluated by measurement of the absorbance at  
25 595 nm.  $\text{IC}_{50}$  values (compound concentration that produces 50% of cell growth inhibition) were  
26 calculated from curves constructed by plotting cell survival (%) versus drug concentration ( $\mu\text{M}$ ). All  
27 experiments were made in triplicate.  
28  
29  
30  
31  
32  
33  
34  
35  
36  
37  
38  
39  
40  
41  
42  
43  
44  
45  
46  
47  
48  
49  
50  
51  
52  
53  
54  
55  
56  
57  
58  
59  
60

## RESULTS AND DISCUSSION

### *Formation and characterisation of the cyclic assemblies*

Reaction of [(cymene)RuCl<sub>2</sub>]<sub>2</sub> with K<sub>2</sub>Hoxonate in a methanolic solution leads to the formation of the dinuclear half-sandwich ruthenium(II) complex [(cymene)<sub>2</sub>Ru<sub>2</sub>(μ-Hoxonato)Cl<sub>2</sub>] (**1a**). **1a** has been structurally characterised by single crystal X-ray diffraction. **1a** crystallizes in the monoclinic space group *P2<sub>1</sub>/c*. Its asymmetric unit consists of two Ru(II) and two chloride ions, one Hoxonato and two cymene moieties, all in general positions. The Hoxonato ligands act in a *N,O,N',O'*-exotetradentate bridging mode, connecting two Ru(II) ions, 5.6 Å apart, within dinuclear [(cymene)<sub>2</sub>Ru<sub>2</sub>(μ-Hoxonato)Cl<sub>2</sub>] complexes (Figure 1). The coordination sphere of each metal ion is completed by one chloride anion and one η<sup>6</sup>-cymene ligand, the chloride ions of the dimer adopting a *trans* disposition with respect to the mean plane formed by the two Ru(II) ions and the Hoxonato moiety. Intermolecular non bonding interactions of the Cl...N kind are present between one of the two chloride anions of the complex and the H(N) hydrogen atom on the Hoxonato ring of an adjacent complex, this imparting further stability to the whole crystal structure.

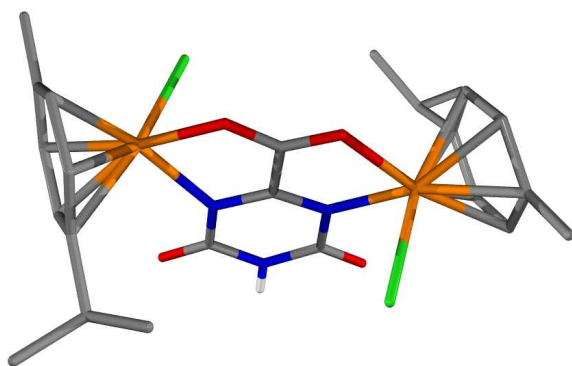
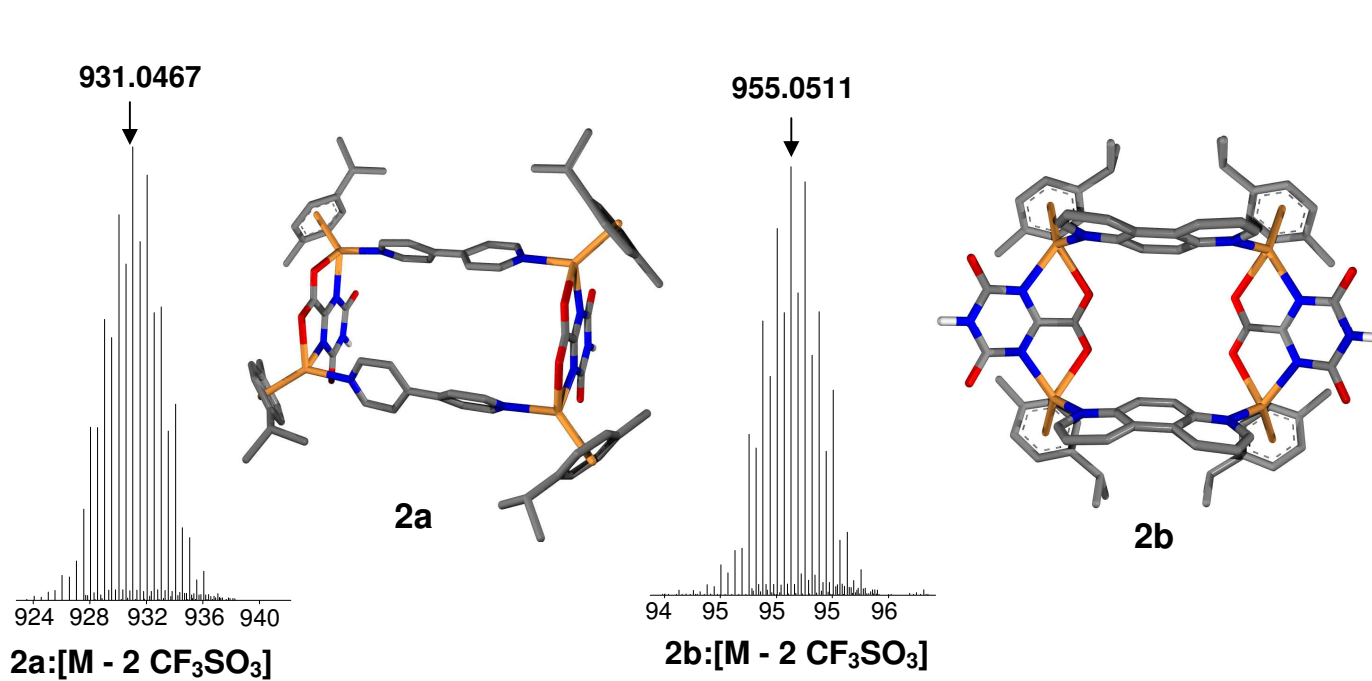
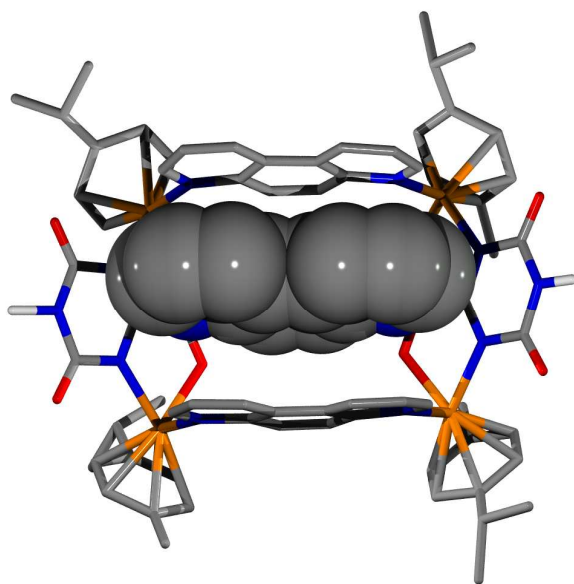


**Figure 1.** Crystal structure of [(cymene)<sub>2</sub>Ru<sub>2</sub>(μ-Hoxonato)Cl<sub>2</sub>] (**1a**). C (grey), N (blue), O (red), Ru (orange), Cl (green). H-atoms with the exception of the NH moiety have been omitted for sake of clarity.



25  
26  
27  
28  
29  
30  
31  
32

*Figure 2.* ESI-MS spectrum and molecular force field model of [(cymene)<sub>4</sub>Ru<sub>4</sub>(Hoxonato)<sub>2</sub>(4,4'-bpy)<sub>2</sub>]<sup>4+</sup> (**2a**) and [(cymene)<sub>4</sub>Ru<sub>4</sub>(Hoxonato)<sub>2</sub>(4,7-phen)<sub>2</sub>]<sup>4+</sup> (**2b**).



53  
54  
55  
56  
57  
58  
59  
60

*Figure 3.* Crystal structure of the supramolecular assembly [(cymene)<sub>4</sub>Ru<sub>4</sub>(Hoxonato)<sub>2</sub>(4,7-phen)<sub>2</sub>]<sup>4+</sup> (**2b-4,7-phen**). C (grey), N (blue), O (red), Ru (orange). H-atoms with the exception of the NH moiety have been omitted for sake of clarity.

1  
2  
3 Removal of the chloride ligands of **1a** by treatment with  $\text{AgCF}_3\text{SO}_3$  leads to the formation of  
4  
5  $[(\text{cymene})_2\text{Ru}_2(\mu\text{-Hoxonato})(\text{CF}_3\text{SO}_3)_2]$  (**1b**) which, upon posterior reaction with the  $N,N'$ -linkers 4,4'-  
6  
7 bpy and 4,7-phen, yields the tetranuclear cage complexes  $[(\text{cymene})_4\text{Ru}_4(\text{Hoxonato})_2(N,N'$   
8  
9  $\text{L})_2](\text{CF}_3\text{SO}_3)_4$  (**2a**: L = 4,4'-bpy; **2b**: L = 4,7-phen) (Scheme 1). These systems have been studied by  $^1\text{H}$   
10  
11 NMR and ESI-MS and their structures have been modeled by molecular force field modeling (Figure 2).  
12  
13 The ESI-MS spectra are unequivocally indicative of the formation of the tetranuclear **2a** and **2b** species.  
14  
15 Noteworthy, the  $[\text{M} - 2\text{CF}_3\text{SO}_3]^{2+}$  peaks correspond in both cases to the most intense ones in the mass  
16  
17 spectra. This feature should be taken as a proof of their high stability. Indeed,  $^1\text{H}$  NMR spectra for these  
18  
19 species in both DMSO- $d_6$  and  $\text{D}_2\text{O}$  remain unaltered for weeks which agrees with the robustness of  
20  
21 these systems in both solvents. Noteworthy, in the case of **2b**, the  $^1\text{H}$  NMR experiments indicate the  
22  
23 presence of two species, which can be attributed to the coexistence of **2b** in its cone and 1,3-alternate  
24  
25 conformations, as confirmed by variable temperature  $^1\text{H}$  NMR measurements, which shows the  
26  
27 stabilization of the 1,3-alternate conformer at high temperature.  
28  
29  
30  
31  
32

33 The X-ray crystal structure investigation on **2b-4,7-phen** shows that this species crystallizes in the  
34  
35 orthorhombic  $P2_12_12_1$  space group and it is composed by rectangular tetranuclear  
36  
37  $[\text{Ru}_4(\text{cymene})_4(\text{Hoxonato})_2(4,7\text{-phen})_2]^{4+}$  cationic open boxes (Figure 3), in which the Hoxonato and  
38  
39 4,7-phen ligands show, respectively,  $N,O,N',O'$ -exotetradentate and  $N^A,N^7$ -exobidentate coordination  
40  
41 modes, bridging Ru(II) centers 5.6 and 7.9 Å apart. The open boxes adopt the cone conformation,  
42  
43 thereby creating a vase-like cavity suitable for molecular recognition processes. Indeed, the wider  
44  
45 entrance of the cone hosts one non-coordinated 4,7-phen molecule, whose shortest atom-atom contacts  
46  
47 with the Hoxonato and 4,7-phen cavity walls are, respectively, 3.0 and 3.2 Å. One methanol molecule is  
48  
49 placed about the opposite entrance of the cone, while two triflate anions are located nearby. The  
50  
51 cohesiveness of the structure is granted also by hydrogen bond interactions of the (N)H $\cdots$ O type (N $\cdots$ O  
52  
53 2.75, 2.76 Å) involving the non bonded nitrogen and oxygen atoms of two Hoxonato ligands belonging  
54  
55 to distinct, nearby complexes. On the whole, each tetramer is hydrogen bonded to two adjacent ones,  
56  
57  
58  
59  
60

1 this creating 1-D zig-zag strands running approximately along [001]. Weaker hydrogen bonds of the  
2 (O)H...O kind (O...O 3.02 Å) are present between the hydroxyl groups of the solvent molecules and the  
3 oxygen atoms of nearby triflate anions.  
4  
5  
6  
7  
8

9 *Reactivity and molecular recognition properties of the Ru(II) assemblies towards biorelevant species*

10 The reactivity of [(cymene)<sub>2</sub>Ru<sub>2</sub>(Hoxonato)Cl<sub>2</sub>] (**1a**) towards mononucleotides was studied in both  
11 DMSO and aqueous solution by <sup>1</sup>H-NMR at room temperature and at pH 7.0. The results show that the  
12 chloride ligands do not exchange neither with the solvent nor with the mononucleotides. The addition of  
13 a nucleotide in deuterated DMSO is responsible for the widening and shifting of the amine proton  
14 resonance of the triazine moiety, which should be indicative of the formation of H-bonding interactions  
15 between the Hoxonato moiety and the purine residues of the mononucleotides in low polar solvents like  
16 DMSO. In contrast to **1a**, [(cymene)<sub>2</sub>Ru<sub>2</sub>(Hoxonato)(CF<sub>3</sub>SO<sub>3</sub>)<sub>2</sub>] (**1b**) readily reacts in aqueous solution  
17 with guanosine monophosphate and adenosine monophosphate to give the corresponding  
18 [(cymene)<sub>2</sub>Ru<sub>2</sub>(Hoxonato)(nucleotide)<sub>2</sub>] adducts.  
19  
20  
21  
22  
23  
24  
25  
26  
27  
28  
29  
30  
31  
32

33 The suitability of compounds **2a** and **2b** to act as receptors of mononucleotides has been essayed as a  
34 preliminary model of their non-covalent interaction with DNA. In this regard, the presence of the  
35 extended aromatic 4,7-phen ligands and the H-bonding features of the Hoxonate moieties suit these  
36 systems for giving stacking and complementary H-bonding interactions with nucleobases.  
37  
38  
39  
40  
41

42 The results show that the addition of a mononucleotide (AMP, GMP) to an aqueous solution of **2a** and  
43 **2b** is only responsible for a slight upfield shift of the <sup>1</sup>H NMR signals, with no observation of ligand  
44 exchange processes. The latter observation is a further proof of the stability of these systems in aqueous  
45 solution. Determination of the association constants for the interaction of **2a** or **2b** with  
46 mononucleotides in aqueous solution was carried out by means of <sup>1</sup>H NMR at pH 7.0.<sup>20</sup> The very low  
47 values  $K_{\text{ass}} < 4 \text{ M}^{-1}$  indicate that the mononucleotides are not incorporated inside the cavity of the  
48 receptors but probably interact with their external surface through H-bonding,  $\pi$ - $\pi$ , anion- $\pi$  and  
49 electrostatic interactions. It is also important to mention that these systems neither react in aqueous  
50  
51  
52  
53  
54  
55  
56  
57  
58  
59  
60

1 solution with S-donor ligands. Indeed, <sup>1</sup>H NMR studies show that incubation of **2a** with 4 equivalents of  
2 cysteine, during two hours at 37 °C at pH 7.4, is not responsible for ligand exchange processes. This  
3 result suggests that S-donor atoms from other biomolecules (i.e. glutathione, proteins) should not  
4 significantly interfere.  
5  
6  
7  
8  
9  
10  
11  
12  
13  
14  
15  
16  
17  
18  
19  
20  
21  
22  
23  
24  
25  
26  
27  
28  
29  
30  
31  
32  
33  
34  
35  
36  
37  
38  
39  
40  
41  
42  
43  
44  
45  
46  
47  
48  
49  
50  
51  
52  
53  
54  
55  
56  
57  
58  
59  
60

## DNA binding assays

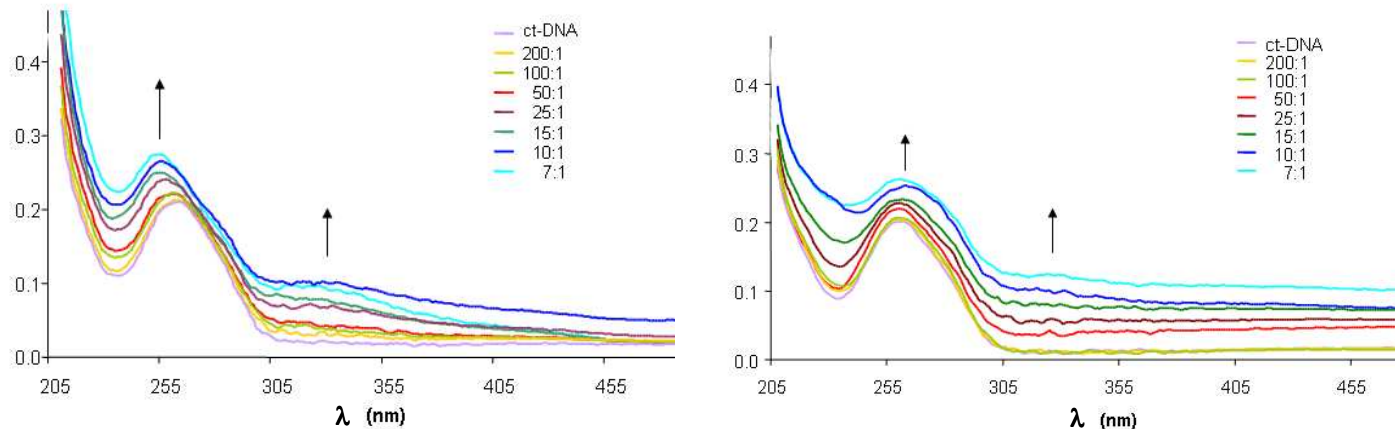


**Figure 4.** Effect of addition of the coordination assemblies  $[(\text{cymene})_4\text{Ru}_4(\text{Hoxonato})_2(4,4'\text{-bpy})_2](\text{CF}_3\text{SO}_3)_4$  (**2a**, left) and  $[(\text{cymene})_4\text{Ru}_4(\text{Hoxonato})_2(4,7\text{-phen})_2](\text{CF}_3\text{SO}_3)_4$  (**2b**, right) to a solution of *ct*-DNA (34  $\mu\text{M}$ ) on the UV-vis spectra in a 200:1 to 7:1 ratio. Subtraction of the coordination assemblies spectra has been made.

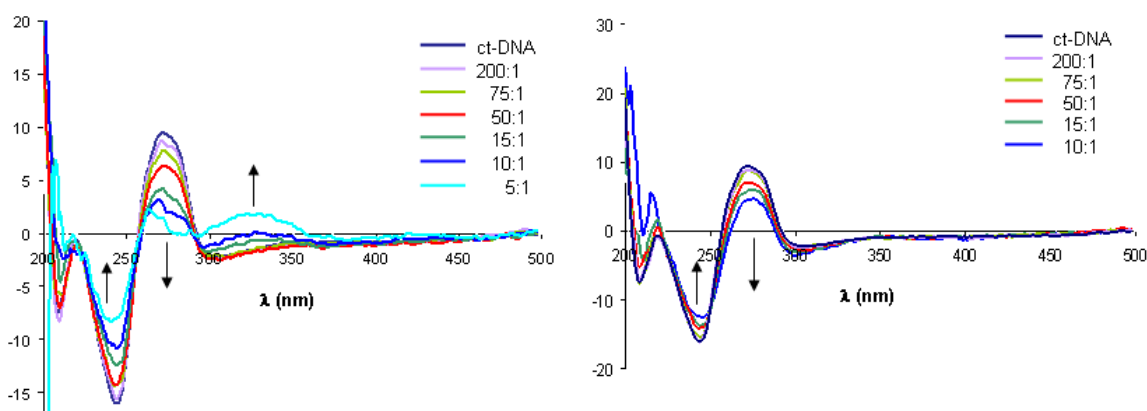


**Figure 5.** CD spectra of the titration of *ct*-DNA (300  $\mu\text{M}$ ) with  $[(\text{cymene})_4\text{Ru}_4(\text{Hoxonato})_2(4,4'\text{-bpy})_2](\text{CF}_3\text{SO}_3)_4$  (**2a**) and  $[(\text{cymene})_4\text{Ru}_4(\text{Hoxonato})_2(4,7\text{-phen})_2](\text{CF}_3\text{SO}_3)_4$  (**2b**) in a 200:1 to 5:1 ratio.



1  
2  
3 UV-visible absorbance (UV-vis), circular dichroism (CD) and ethidium bromide (EB) competitive  
4 binding assays were performed in order to assess the capability of these systems to non-covalently bind  
5 to DNA. The results indicate that both **2a** and **2b** do efficiently interact with *ct-DNA*. The UV-vis  
6 spectra show an increase in intensity of the characteristic DNA absorption band ( $\lambda = 260$  nm) upon  
7 complex addition (Figure 4). Conversely, the CD spectra (Figure 5) show a significant decrease of the  
8 signal ellipticity as a consequence of the same interaction, particularly in the case of the interaction of **2a**  
9 with DNA. These results might be indicative of conformational changes in the double strand of DNA as  
10 consequence of a supramolecular interaction between the cyclic systems and DNA.<sup>10</sup> In addition, we  
11 observe, in the case of the interaction of **2a** with DNA, a complex induced band ( $\lambda = 325$  nm), which  
12 should be taken as a further evidence of the interaction of these systems to DNA. In contrast, **1b** is only  
13 responsible for a slight diminution of the characteristic DNA absorption band despite its capability to  
14 covalently bind to DNA. AFM imaging experiments on the interaction of **2a** and **2b** with DNA also  
15 suggest that the interaction of these systems induce significant changes in the shape of the DNA strands,  
16 namely stiffening along with strand aggregation (cross-links) (Figure 6). This type of behavior is in  
17 contrast with the DNA coiling induced by Hannon's metallocylinders major groove binders,<sup>8</sup> but can be  
18 related to the conformational changes induced by platinum(II) metallacalixarenes.<sup>10</sup> Taking into account  
19 charge, size and shape considerations, **2a** and **2b** should also fit into the DNA major groove inducing a  
20 concomitant distortion in the DNA structure.<sup>21</sup> Moreover, competitive binding assays show a slight  
21 diminution in the fluorescence of EB upon complex addition (see Supporting Information). This could  
22 be related to the displacement of the EB slotted in the DNA major groove in presence of these  
23 complexes.  
24  
25  
26  
27  
28  
29  
30  
31  
32  
33  
34  
35  
36  
37  
38  
39  
40  
41  
42  
43  
44  
45  
46  
47  
48  
49  
50  
51  
52  
53  
54  
55  
56  
57  
58  
59  
60

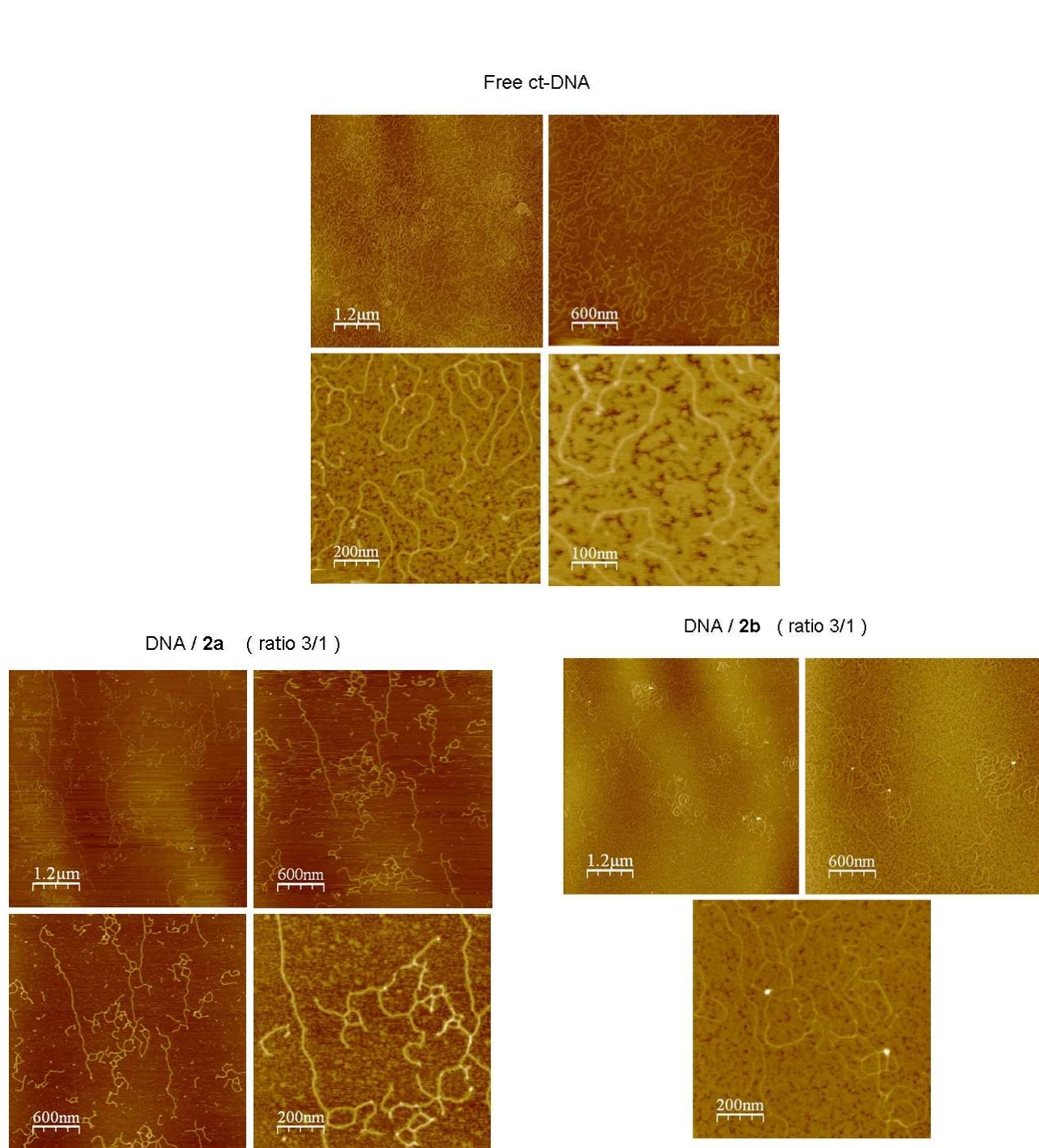


Figure 6. AFM images of free ct-DNA (top) and ct-DNA-complexes (ct-DNA-**2a** (left down) and ct-DNA-**2b** (right down)) at DNA base pairs: complex 3:1 ratio.

### *Cytotoxicity studies*

To explore the potential biological effects of the interaction of these systems with biomolecules, we have evaluated their cytotoxicity on human lung NCI-H460, human ovarian A2780 and A2780cisR

1 cancer cell lines. IC<sub>50</sub> data are reported in Table 2. These systems are not active towards the lung  
2 carcinoma NCI-H460 cell line. In the case of the ovarian A2780 cancer cells, it is interesting to observe  
3 that, while compound **1a** is not active, compounds **1b**, **2a** and **2b** show cytotoxic activity against this  
4 cell line, although the activities are 20-30 times lower than those exhibited by *cisplatin*. Noteworthy, the  
5 activity of **1b**, **2a** and **2b** systems towards the A2780cisR cancer cell line with acquired resistance to  
6 *cisplatin* is significantly higher, which give rise to unusually low RF values.<sup>22</sup> The lack of cytotoxic  
7 activity of **1a** was expected in view of its inertness to exchange processes (see above); by contrast, the  
8 activity of compounds **2a** and **2b** towards A2780 cancer cell line is quite striking in view of the non-  
9 covalent nature of their interaction to DNA. Moreover, their high activity towards the *cisplatin* resistant  
10 A2780cisR cancer cell line and the very low resistance factors (RF) might be indicate efficient  
11 circumvention of *cisplatin* resistance.<sup>23</sup> On the other hand the poor activity of these systems towards the  
12 lung NCI-H460 cell line might be indicative of a low toxicity of these systems, These features might be  
13 taken as a proof of a differentiated mechanism of action of **2a** and **2b** with respect to classical  
14 metallodrugs. In this regard, it should be noted that ruthenium metallodrugs, that are currently in clinical  
15 trials (NAMI-A and KP1019), like *cisplatin*, possess chloride ligands that can be exchanged in order to  
16 bind to biomolecules. It is therefore of high interest to find systems with alternative mechanisms of  
17 action. Non-covalent binding of metallodrugs to DNA is an attractive approach; however, most of the  
18 effort has been focused on intercalators, with a few exceptions being Hannon's major groove binders of  
19 metalocyclinder type<sup>6</sup> and our recent report on platinum(II) metallacalixarenes.<sup>8,9</sup>

## 47 CONCLUSIONS

48 We have prepared a series of robust organometallic/coordination Ru(II) cyclic assemblies which do  
49 not give ligand exchange reactions neither with N-donor biorelevant ligands (nucleobases), nor with S-  
50 donor biorelevant ligands (cysteine) in aqueous solutions. Nevertheless, these systems are able to  
51 interact non-covalently with DNA, inducing significant conformational changes in this biomolecule.  
52 These results also imply that different supramolecular drug designs might be used to induce different  
53  
54  
55  
56  
57  
58  
59  
60

1 DNA structural effects. Moreover, the cytotoxic activity towards *cisplatin* resistant cancer cells suggests  
2 that metal coordination assemblies able to bind non-covalently to biomolecules may be a very promising  
3 field of research, which may circumvent the heavy metal accumulation problems of platinum and related  
4 metallodrugs. It should also be highlighted that the inactivity of these systems towards lung carcinoma  
5 NCI-H460 cell lines might be indicative that this kind of systems are not highly cytotoxic and might be  
6 selective towards specific cell lines.  
7  
8

9  
10  
11  
12  
13  
14 Work is in progress in order to systematically control the shape and size of this kind of assemblies and  
15 to study if there is a DNA binding sequence specificity.  
16  
17  
18  
19  
20

21  
22 **Acknowledgments.** Funding from the Spanish Ministerio de Educación y Ciencia (CTQ2005-  
23 00329/BQU), Junta de Andalucía, Universidad de Granada (Contrato de Incorporación de Doctores  
24 (EB)), the Marie Curie program (MAG) and COST-D39 Action are acknowledged.  
25  
26  
27  
28  
29

30  
31 **Supporting Information Available.** <sup>1</sup>H NMR, UV-vis, CD and Fluorescence spectra which can be  
32 obtained from <http://pubs.acs.org>.  
33  
34  
35  
36  
37  
38  
39  
40  
41  
42  
43  
44  
45  
46  
47  
48  
49  
50  
51  
52  
53  
54  
55  
56  
57  
58  
59  
60

**Table 1:** Crystallographic data and refinement parameters for species **1a** and **2b-c4,7-phen**.

	<b>1a</b>	<b>2b-c4,7-phen</b>
formula	C <sub>24</sub> H <sub>28</sub> Cl <sub>2</sub> N <sub>3</sub> O <sub>4</sub> Ru <sub>2</sub>	C <sub>89</sub> H <sub>88</sub> F <sub>12</sub> N <sub>12</sub> O <sub>21</sub> Ru <sub>4</sub> S <sub>4</sub>
<i>FW</i> (g mol <sup>-1</sup> )	695.5	2422.3
<i>T</i> (K)	298(2)	100(2)
$\lambda$ (Å)	0.71073	0.71073
crystal system	Monoclinic	orthorhombic
space group	<i>P</i> 2 <sub>1</sub> / <i>c</i>	<i>P</i> 2 <sub>1</sub> 2 <sub>1</sub> 2 <sub>1</sub>
<i>a</i> (Å)	12.609(2)	14.1402(5)
<i>b</i> (Å)	12.810(4)	21.9479(6)
<i>c</i> (Å)	16.720(6)	30.7251(9)
$\alpha$ (deg)	90	90
$\beta$ (deg)	107.35(2)	90
$\gamma$ (deg)	90	90
<i>V</i> (Å <sup>3</sup> )	2578(1)	9535.5(5)
<i>Z</i>	4	4
$\rho$ (calc) (Mg m <sup>-3</sup> )	1.415	1.687
$\mu$ (Mo-K $\alpha$ , mm <sup>-1</sup> )	1792	0.810
<i>F</i> (000)	1388	4888
Sample Size (mm <sup>3</sup> )	0.10×0.10×0.05	0.24×0.18×0.14
2 $\theta$ range (deg)	6.0 – 50.6	2.28 - 52.8
<i>hkl</i> range	-15 ≤ <i>h</i> ≤ 14 -3 ≤ <i>k</i> ≤ 15 -8 ≤ <i>l</i> ≤ 20	-17 ≤ <i>h</i> ≤ 17 -27 ≤ <i>k</i> ≤ 27 -38 ≤ <i>l</i> ≤ 38
unique, observed reflections	4678, 3025	19586, 18078
<i>R</i> (int), <i>R</i> (sigma)	0.008, 0.085	0.056, 0.036
data, restraints, parameters	4678, 0, 316	19586, 0, 1102
$\chi$ ( <i>F</i> <sup>2</sup> ) <sup>a</sup>	1.044	1.611
<i>R</i> ( <i>F</i> ), <i>wR</i> ( <i>F</i> <sup>2</sup> ) for <i>I</i> > 2 $\sigma$ ( <i>I</i> ) <sup>[a]</sup>	0.052, 0.087	0.065, 0.193
<i>R</i> ( <i>F</i> ), <i>wR</i> ( <i>F</i> <sup>2</sup> ) for all reflections <sup>[a]</sup>	0.103, 0.102	0.071, 0.197
highest peak, deepest hole (e Å <sup>-3</sup> )	0.653, -0.611	4.01, -1.65

<sup>[a]</sup>  $\chi(F^2) = [\sum w(F_o^2 - F_c^2)^2 / (n - p)]^{1/2}$  where *n* is the number of reflections, *p* the number of parameters and  $w = 1/[\sigma^2(F_o^2) + (0.019P)^2 + 1.88P]$  with  $P = (F_o^2 + 2F_c^2)/3$ .  $R(F) = \sum |F_o| - |F_c| / \sum |F_o|$  and  $wR(F^2) = [\sum w(F_o^2 - F_c^2)^2 / \sum w F_o^4]^{1/2}$ .

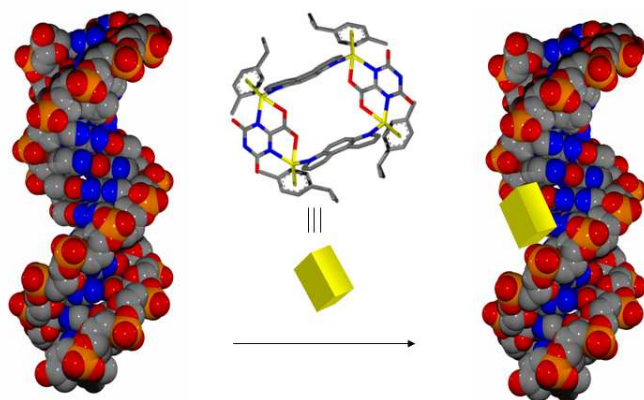
**Table 2.** IC<sub>50</sub><sup>a</sup> values (in μM) in lung NCI-H460, ovarian A2780 and *cisplatin* resistant A2780*cisR* cancer cell lines and resistance factor RF (IC<sub>50</sub> *cisplatin* resistant / IC<sub>50</sub> *cisplatin* sensitive).

Compound <sup>[a]</sup>	NCI-H460	A2780	A2780 <i>cisR</i>	RF
<b>1a</b>	>100 μM	>100 μM	>100 μM	-
<b>1b</b>	-	20	2.4	0.12
<b>2a</b>	>100 μM	19	4.6	0.24
<b>2b</b>	>100 μM	15	8.3	0.55
<b><i>Cisplatin</i></b>	5.7	0.66	3.7	5.61

<sup>a</sup> IC<sub>50</sub> : drug concentration necessary for 50% inhibition of cell viability.

## SYNOPSIS TOC

Robust tetracationic ruthenium(II) cyclic systems are able to bind non-covalently to the major groove of DNA inducing conformational changes in this biomolecule, and exhibit cytotoxic activity towards ovarian cancer cell line with acquired *cisplatin* resistance A2780*cisR*.



## REFERENCES

- 1  
2  
3  
4  
5  
6  
7  
8  
9  
10  
11  
12  
13  
14  
15  
16  
17  
18  
19  
20  
21  
22  
23  
24  
25  
26  
27  
28  
29  
30  
31  
32  
33  
34  
35  
36  
37  
38  
39  
40  
41  
42  
43  
44  
45  
46  
47  
48  
49  
50  
51  
52  
53  
54  
55  
56  
57  
58  
59  
60
- 
- <sup>1</sup> Cisplatin, Chemistry and Biochemistry of A Leading Anti-Cancer Drug (Ed.: Lippert, B.), Wiley-VCH, Weinheim, 1999.
- <sup>2</sup> Aird, R.; Cummings, J.; Ritchie, A.; Muir, M.; Morris, R.; Chen, H.; Sadler, P.; Jodrell, D. *Br. J. Cancer* **2002**, *86*, 1652-1657.
- <sup>3</sup> Galindo, M. A.; Quirós, M.; Romero, M. A.; Navarro, J. A. R. *J. Inorg. Biochem.* **2008**, *102*, 1025-1032.
- <sup>4</sup> Yan, Y.K.; Melchart, M.; Habtemariam, A.; Sadler, P.J. *Chem. Commun.* **2005**, 4764-4776.
- <sup>5</sup> a) Ang, W. H.; Dyson, P. J. *Eur. J. Inorg. Chem.* **2006**, 4003-4018; b) Hannon, M.J. *Pure and Applied Chemistry*, **2007**, *79*, 2243-2261.
- <sup>6</sup> Therrien, B.; Süss-Fink, G.; Govindaswamy, P.; Renfrew, A. K.; Dyson, P. J. *Angew. Chem. Int. Ed.* **2008**, *47*, 3773-3776.
- <sup>7</sup> a) Hannon, M.J.; Moreno, V.; Prieto, M.J.; Molderheim, E.; Sletten, E.; Meistermann, I.; Isaac, C.J.; Sanders, K.J.; Rodger, A. *Angew. Chem., Intl. Ed.*, **2001**, *40*, 879-884; b) Hotze, A.C.G.; Hodges, N.J.; Hayden, R.E.; Sanchez-Cano, C.; Paines, C.; Male, N.; Tse, M.-K.; Bunce, C.M.; Chipman, J.K.; Hannon, M.J. *Chemistry & Biology*, **2008**, *15*, 1258-1267; c) M.J. Hannon, *Chem. Soc. Rev.*, **2007**, *36*, 280-295.
- <sup>8</sup> Pascu, G. I.; Hotze, A. C. G.; Sanchez-Cano, C.; Kariuki, B M.; Hannon, M. J. *Angew. Chem. Int. Ed.* **2007**, *46*, 4374-4378.
- <sup>9</sup> a) Mounir, M.; Lorenzo, J.; Ferrer, M.; Prieto, M. J.; Rossell, O.; Aviles, F. X.; Moreno, V. *J. Inorg. Biochem.* **2007**, *101*, 660-666; b) Kieltyka, R.; Englebienne, P.; Fakhoury, J.; Autexier, C.; Moitessier, N.; Sleiman, H. F. *J. Am. Chem. Soc.* **2008**, *130*, 10040-10041.
- <sup>10</sup> Galindo, M. A.; Olea, D.; Romero, M. A.; Hannon, M. J.; Rodger, A.; Gómez, J.; del Castillo, P.; Zamora, F.; Navarro, J. A. R. *Chem. Eur. J.* **2007**, *13*, 5075-5081.



- 1  
2  
3  
4  
5  
6  
7  
8  
9  
10  
11  
12  
13  
14  
15  
16  
17  
18  
19  
20  
21  
22  
23  
24  
25  
26  
27  
28  
29  
30  
31  
32  
33  
34  
35  
36  
37  
38  
39  
40  
41  
42  
43  
44  
45  
46  
47  
48  
49  
50  
51  
52  
53  
54  
55  
56  
57  
58  
59  
60
- <sup>11</sup> Galindo, M. A.; Romero, M. A.; Navarro, J. A. R. *Inorg. Chim. Acta* **2009**, *362*, 1027-1030.
- <sup>12</sup> Sawada, T.; Yoshizawa, M.; Sato, S.; Fujita, M. *Nature Chem.* **2009**, *1*, 53-56.
- <sup>13</sup> a) Gamez, P.; Mooibroek, T. J. ; Teat, S. J.; Reedijk, J. *Acc. Chem. Res.* **2007**, *40*, 435-444; b) Schottel, B. L.; Chifotides, H. T; Dunbar, K. R. *Chem. Soc. Rev.* **2008**, *37*, 68–83.
- <sup>14</sup> Schlawe, D.; Majdalani, A.; Velcicky, J.; Heßler, E.; Wieder, T.; Prokop, A.; Schmalz, H.-G. *Angew. Chem. Int. Ed.* **2004**, *43*, 1731–1734.
- <sup>15</sup> Komiya, S. *Synthesis of Organometallics Compounds*, John Wiley & Sons, 1997 (Chapter 8).
- <sup>16</sup> North, A. T. C.; Phillips, D. C.; Mathews, F. S. *Acta Cryst.* **1968**, *A24*, 351-359.
- <sup>17</sup> SIR97, Altomare, A.; Burla, M. C.; Camalli, M.; Cascarano, G. L.; Giacovazzo, C.; Guagliardi, A.; Moliterni, A. G. G.; Polidori, G.; Spagna, R. *J. Appl. Crystallogr.* **1999**, *32*, 115.
- <sup>18</sup> Sheldrick, G. M. SHELX-97, Program for crystal structure determination, 1997, University of Göttingen, Göttingen, Germany.
- <sup>19</sup> Sheldrick, G. M. SADABS, software for empirical absorption correction, 1996, University of Göttingen, Göttingen, Germany.
- <sup>20</sup> Galindo, M. A.; Galli, S.; Navarro, J. A. R.; Romero, M. A. *Dalton Trans.* **2004**, 2780-2785.
- <sup>21</sup> Approximate dimensions for **2a** and **2b** are 2 nm x 1.5 nm x 0.7 nm and 1.5 nm x 1.5 nm x 0.8 nm, respectively.
- <sup>22</sup> Ruiz, J.; Lorenzo, J.; Vicente, C.; López, G.; López de Luzuriaga, J. M.; Monge, M.; Avilés, F. X.; Bautista, D.; Moreno, V.; Laguna, A. *Inorg. Chem.* **2008**, *47*, 6990-7001.
- <sup>23</sup> Ruiz, J.; Rodríguez, V.; Cutillas, N.; López, G.; Bautista, D. *Inorg. Chem.* **2008**, *47*, 10025-10036.



---

1  
2  
3  
4  
5  
6  
7  
8  
9  
10  
11  
12  
13  
14  
15  
16  
17  
18  
19  
20  
21  
22  
23  
24  
25  
26  
27  
28  
29  
30  
31  
32  
33  
34  
35  
36  
37  
38  
39  
40  
41  
42  
43  
44  
45  
46  
47  
48  
49  
50  
51  
52  
53  
54  
55  
56  
57  
58  
59  
60